1996ApJ...459..773D

THE ASTROPHYSICAL JOURNAL, 459:773–778, 1996 March 10
No copyright is claimed for this article. Printed in U.S.A.

THE TEMPERATURE OF THE BRIGHT KNOTS AT THE TOPS OF SOLAR FLARE LOOPS

G. A. DOSCHEK AND U. FELDMAN
E. O. Hulburt Center for Space Research, Naval Research Laboratory, Washington, DC 20375-5352
Received 1995 July 6; accepted 1995 September 20

ABSTRACT

The Japanese *Yohkoh* spacecraft has revealed the pervasive presence of confined bright regions at the tops of solar flare magnetic flux tubes. The physical parameters in the bright regions, such as temperature and density, are of considerable interest for attempting to understand the nature and longevity of these regions. We have found an example of such a source in spectroheliograms of a flare observed by the Naval Research Laboratory slitless spectroheliograph on *Skylab*. This instrument offers better temperature discrimination than possible with a broadband X-ray telescope such as flown on *Yohkoh*. We determine the temperature of the *Skylab* source using the most recent atomic data. From the *Skylab* extreme-ultraviolet images of this flare in spectral lines of Fe XXII, Fe XXIII, and Fe XXIV, we find that the confined bright region can be described as an isothermal source at a temperature of about 11×10^6 K. However, this conclusion generally contradicts temperatures measured from uncollimated Bragg crystal spectrometer spectra from *Yohkoh* and other spacecraft for similar X-ray class flares. There is also emission at the same location from Ca XVII ions formed at about 6×10^6 K, implying that the source might be multithermal. A multithermal source would indicate that the bright regions are composed of structures below the spatial resolution of the *Skylab* and *Yohkoh* instrumentation and could possibly resolve the discrepancies between Bragg spectrometer and imaging data.

Subject headings: MHD — Sun: flares — Sun: UV radiation

1. INTRODUCTION

A perplexing discovery from the Japanese *Yohkoh* high-energy solar physics spacecraft is the confined soft X-ray (SXR) bright regions that appear at the tops of magnetic flux tubes (loops) that contain the SXR-emitting flare plasma (e.g., Acton et al. 1992; Feldman et al. 1994; Doschek, Strong, & Tsuneta 1995). These regions appear at the tops of many flaring loops, including both compact flares and long duration events (LDEs). They are most striking in LDEs (e.g., Feldman et al. 1995) and were previously noticed in a few LDE *Skylab* events (Kahler 1977; Vorpahl, Tandberg-Hanssen, & Smith 1977). However, it is the *Yohkoh* observations that have drawn the attention of the solar flare community to the pervasiveness of the bright regions in flares.

An illustration of a compact flare bright region is shown in Figure 1 (Plate 31). The flare images were recorded by the soft X-ray telescope (SXT) on *Yohkoh* (see Tsuneta et al. 1991 for a description of the instrument). This X-ray class M2 event occurred on the limb on 1992 January 13 near 17:30 UT. The left panel in Figure 1 shows the loop top early in the rise phase, when a footpoint region brightening is also apparent. The right panel shows the flare loop near flare maximum, when the loop-top brightening is the dominant feature of the flare loop. The intensity/time behavior of the loop top for this particular event is illustrated quantitatively in Doschek et al. (1995) (see Fig. 10 in that paper).

The bright region in Figure 1 could be understood in a straightforward way if the plasma pressure in it were equal to the pressure outside it, i.e., in the legs of the loop. (It appears from inspection of many flares that a geometric projection effect cannot account for the bright regions, although projection effects may be important in deducing certain quantitative information about the bright regions.) Otherwise, the bright region is conceptually difficult to understand because both mass and energy are freely transported along magnetic field lines, and therefore a confined region involving a pressure gradient in a magnetic flux tube should exist for only a very short time. However, regions such as shown in Figure 1 can last for much of a compact flare's lifetime (on the order of tens of minutes) and for many hours in an LDE.

Measurement of the plasma pressure involves knowing both the electron temperature and density in the loop, including the bright region. Thus, these plasma parameters are crucial for understanding the physics of the regions.

The electron density in the bright regions was determined by Doschek (1994) and Doschek et al. (1995) for a few representative cases, ignoring projection effects. The derived densities are high, on the order of 5×10^{10}–10^{12} cm^{-3}. These densities are typical of those derived from high spatial resolution *Skylab* observations, and therefore the bright regions do not appear to be underdense relative to the legs of the loop. The bright region can only have a lower pressure than the legs of the loop if it has a lower temperature than the loop legs, i.e., if it is a condensation.

The electron temperature of the bright regions has been measured by McTiernan et al. (1993) using SXR images obtained by SXT. Doschek et al. (1995) and Feldman et al. (1995) have obtained similar results with SXT data. The SXT derived temperature of the bright region for M class events is in many cases around 12×10^6 K. McTiernan et al. (1993) reported that higher temperature regions are found in fainter regions adjacent to, but outside the loop containing the bright region. The higher temperatures can be 15–25×10^6 K and are similar to those found from X-ray iron line spectra obtained from a Bragg crystal spectrometer (BCS) experiment on *Yohkoh* (see Culhane et al. 1991 for a description of the instrument) as well as from many previous Bragg spectrometer experiments on other spacecraft (e.g., see Doschek 1990). McTiernan et al. (1993), Doschek et

© American Astronomical Society • Provided by the NASA Astrophysics Data System

1996ApJ...459..773D

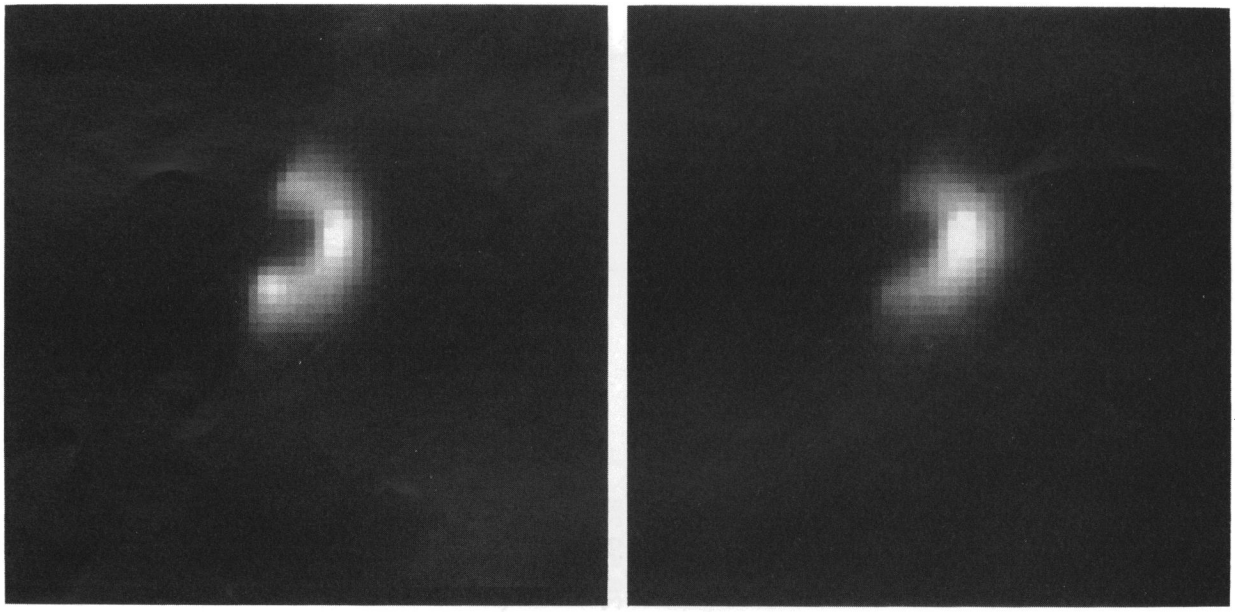

FIG. 1.—*Yohkoh* example of a bright region at the top of a flare loop. The flare occurred on 1992 January 13 and is discussed by Doschek et al. (1995). The solar dimensions of each panel are 68,250 × 68,250 km^2. The left panel was obtained during the flare rise phase; the right panel was obtained near maximum flux. The flare was observed above the solar limb.

© American Astronomical Society • Provided by the NASA Astrophysics Data System

1996ApJ...459..773D

al. (1995), and Feldman et al. (1995) find that there is little variation on SXT temperature along the loop. Thus, the pressure of the combined bright regions is higher than in the legs over extended time intervals, thereby eliminating a simple explanation for the bright regions.

The SXT flare temperature of the bright loop tops is significantly less than the iron spectra electron temperature obtained from the BCS and earlier spectrometers. Typical BCS iron spectra temperatures are 20×10^6 K, and it is important to determine if some of this temperature plasma resides in loop structures that are bright in SXT flare images or instead resides only in the fainter regions outside of but close to the bright SXT structures, as discussed by McTiernan et al. (1993). Because different techniques are used to determine SXT and BCS temperatures, and the two instruments are sensitive in different wavelength bands, it is not obvious how to compare temperatures or reconcile differences in temperatures determined from the two instruments. Furthermore, a multithermal plasma complicates the interpretation of temperatures because temperatures are determined from SXT and BCS assuming an isothermal plasma. Thus, these temperatures are averaged over the emission measure (along the line of sight for SXT and of the entire flare for BCS), and the averaging is different for the two instruments. Because BCS is uncollimated, the locations of all the BCS sources of 20×10^6 K emission in a particular flare are unclear from *Yohkoh* data alone. The fact that BCS is uncollimated is not responsible for the temperature differences between SXT and BCS.

As a specific example, consider the *Yohkoh* event in Figure 1. The maximum value during the flare lifetime of the total emission measure obtained from the SXT images for plasma at temperatures between 16×10^6 K and 25×10^6 K is about 1.3×10^{49} cm^{-3}. The temperature range is typical for BCS temperatures derived for different times over the lifetime of a flare, and because the SXT emission measure is summed over all high-temperature pixels, the result can be compared with the uncollimated BCS iron spectrometer emission measure, which is only sensitive to these high temperatures. However, the maximum BCS emission measure deduced from the iron spectra is about 7×10^{49} cm^3, significantly larger than the corresponding SXT emission measure. Furthermore, the high temperatures measured by SXT occur above the main bright loop apparent in Figure 1. The highest temperature during the flare observations derived for the brightest pixel in the confined loop top in Figure 1 is about 12.5×10^6 K, well below the iron spectra temperatures. It is difficult to accept the low SXT temperatures for the bright loop tops, in view of the large BCS emission measures derived for higher temperature plasma. Another argument against the low SXT temperatures are the average temperatures obtained from BCS Ca XIX spectra, which are usually significantly greater than 12×10^6 K, although less than typical Fe XXV temperatures (Doschek 1990). The Ca XIX emission measures are also quite large.

The presence of emission from the Li-like ion Fe XXIV in Naval Research Laboratory *Skylab* spectroheliograms obtained in the extreme-ultraviolet (EUV) is consistent with the idea that the bright regions in flare loops might contain substantially hotter plasma than indicated by SXT (e.g., Widing & Dere 1977). Li-like ions have a high temperature tail, i.e., they can produce substantial emission at temperatures significantly greater than the temperature at which they have maximum ion abundance in ionization equilibrium.

We attempt to shed light on the temperature of the bright loop top by analyzing three spectral line images recorded in *Skylab* spectroheliograms from a flare that occurred on 1973 June 15 and was discussed previously by a number of authors (e.g., Widing & Dere 1977; Cheng 1977). This flare is a compact event observed near maximum flux and in the decay phase, and it appears to have a bright loop top. We derive temperatures from the intensity ratios of spectral images. We compare the temperatures derived from the *Skylab* flare to the temperatures found for similar X-ray class *Yohkoh* events such as illustrated in Figure 1.

2. THE *SKYLAB* SPECTROHELIOGRAMS

The Naval Research Laboratory spectroheliograph on *Skylab* (called S082-A) was an instrument that imaged the Sun in different EUV emission lines. This was accomplished by using only one optical element, a gold-coated grating with a spherical curvature. The surface curvature of the grating provided imaging with a spatial resolution of about 2″ close to the normal of the grating. The dispersed images of the entire Sun in different spectral emission lines were recorded on film at the focal plane. The instrument is described in detail by Tousey et al. (1977).

The use of film as a detector limited the dynamic range of S082-A as well as the time resolution, and the launch of *Skylab* during a time of solar minimum limited the number of flares observed by the instrument. Nevertheless, the combination of both high spectral and spatial resolution over an extended wavelength range (about 170–630 Å) is still unique in solar space instrumentation and provides much more temperature discrimination than a SXR telescope, which is sensitive to either a blended broad range of temperatures (grazing incidence) or to only a few selected temperatures (normal incidence multilayer optics). Although the S082-A images of extended structures frequently overlap along the direction of dispersion, images of flares generally do not overlap because of their small spatial size.

The flare of 1973 June 15 was one of the best observed compact flares with S082-A. The highest temperature spectral images available are in the doublet lines of Fe XXIV at 192.04 and 255.10 Å. However, fainter images in the spectra, clearly due to hot plasma in the same apparent spatial location as the Fe XXIV–emitting plasma, were also observed and eventually identified in the *Skylab* era as being due to intersystem transitions in Fe XXI, Fe XXII, and Fe XXIII. The Fe XXIV lines emit most strongly at a temperature of about 15×10^6 K and higher, and therefore they could be arising from the same plasma sources as the Fe XXV emission observable from the BCS iron line spectrometer. As mentioned, because Fe XXIV is Li-like, the fractional ion abundance as a function of temperature is asymmetric around the maximum ion abundance, favoring emission at temperatures above 15×10^6 K relative to temperatures below 15×10^6 K. The Fe XXIII line at 263.76 Å is formed in a slightly lower temperature plasma than 15×10^6 K. The Fe XXI and Fe XXII lines (242.07 Å and 247.19 Å, respectively) are formed most efficiently between about 8×10^6 K and 12×10^6 K. These temperatures are based on the ionization equilibrium temperatures of Arnaud & Rothenflug (1985) and Arnaud & Raymond (1992).

The Fe XXI line is very weak, and therefore it is difficult to

© American Astronomical Society • Provided by the NASA Astrophysics Data System

1996ApJ...459..773D

derive accurate intensities for the images. The Fe XXII line is formed at a substantially lower temperature than Fe XXIV, but it is sufficiently intense for the derivation of reliable intensities from a few spectroheliograms. Reliable intensities can also be derived from the Fe XXIII line. A comparison of the spatial relationship of the Fe XXII, Fe XXIII, and Fe XXIV images and their relative intensities therefore provides information on the temperature distribution in the bright loop top.

A measure of the emitting efficiency of a spectral line as a function of electron temperature is the product of the number density of the ion at a particular temperature times the electron impact collisional excitation rate coefficient at the same temperature. This product is often referred to as the contribution function of the spectral line. The excitation rate coefficient has an approximate temperature dependence given by $\exp(-\Delta E/kT_e)/T_e^{1/2}$, where ΔE is the transition energy. The number densities (ionization fractions) obtained from Arnaud & Raymond (1992) are shown in Figure 2 for the Fe XXII, Fe XXIII, and Fe XXIV lines. The functional behavior of the ionization fractions is similar to the contribution function behavior with temperature, for the long-wavelength lines in question. Note the high-temperature tail for the Fe XXIV line, and note also the considerable overlap of the ionization fractions, which implies that all three lines might be observed in an isothermal source. The intensity ratios (in ergs) of the Fe XXII and Fe XXIII lines to the Fe XXIV line are shown in Figure 3 (assuming an isothermal source; see the following section for atomic physics details), for both the Arnaud & Rothenflug and Arnaud & Raymond calculations. For a given ratio, the Arnaud & Raymond (1992) results give a slightly higher temperature than the Arnaud & Rothenflug (1985) calculations.

The 1973 June 15 flare was an X-ray class M3 flare that occurred at N18, W32. It was first observed in the rise phase just prior to flare maximum, and spectroheliograms were recorded during this part of the rise phase, at peak emission, and well into the decay phase. Detailed analyses of the morphology of the June 15 flare were published by Widing & Dere (1977) and Cheng (1977). The morphology of the flare was not simple, but there is a compact bright region in

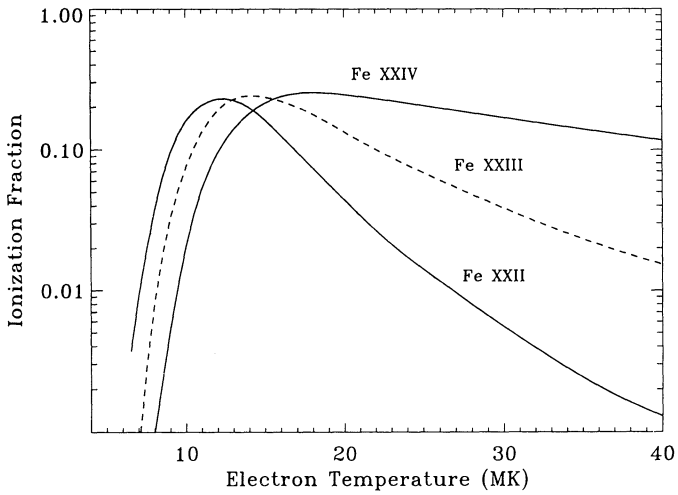

FIG. 2.—Ionization fractions for the 247.19 Å Fe XXII line, the 263.76 Å Fe XXIII line, and the 255.10 Å Fe XXIV line (from Arnaud & Raymond 1992).

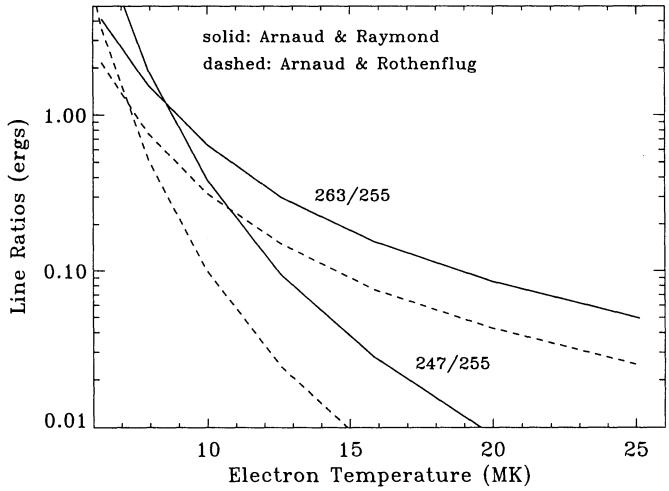

FIG. 3.—Line intensity ratios for the indicated lines for an isothermal plasma. The values of β in eq. (2) are set equal to unity.

the emission lines of Fe XXI–Fe XXIV that appears very similar to the bright regions observed for *Yohkoh* flares. The flare images from all these highly ionized iron ions are co-spatial. During the rise phase, one of the Fe XXIV images (14:11 UT) shows a looplike structure with the brightest emission at the loop top. This region shifts in position as the flare develops, and multiple loop structures are seen in cooler lines during the decay phase, but these types of phenomena are also typical of *Yohkoh* events.

Two Fe XXIV images of the June 15 flare are shown in the upper half of Figure 4 (Plate 32). The upper left panel was one of the first images recorded, but not as early in time for the June 15 flare as for the January 13 flare in Figure 1. The upper right panel in Figure 4 was obtained near flare maximum. The image just to the left of center in each upper panel is the 255 Å Fe XXIV image of the flare. The loop is oriented roughly in the up/down direction in the panels. The image at the right edge of each upper panel is part of the 256 Å He II image of the flare. The brightest areas of the He II image are not co-spatial with the Fe XXI–Fe XXIV images. Note that in the upper right panel, the Fe XXIV image has become more compact and round in appearance because the bright loop top is dominating the emission, as in the right panel of Figure 1. Other interesting details in the panels are discussed by Widing & Dere (1977) and are not repeated here. The images in Figure 4 look very much like a typical *Yohkoh* bright loop-top event, although the loop-top brightening is not as obvious in the *Skylab* images as in the *Yohkoh* images shown in Figure 1. If many of these observations had been available from *Skylab*, the importance of this feature would have been realized from analysis of the *Skylab* spectroheliograms.

As further examples, Fe XXII and Fe XXIII images are shown in the lower left and lower right panels of Figure 4, respectively. The Fe XXII image looks more compact than the other images because it is much weaker and can only be seen in the brightest part of the confined loop top. The Fe XXII image confirms that the loop top is indeed the brightest part of the loop, as for the *Yohkoh* event in Figure 1. The Fe XXIII image is similar in appearance to the Fe XXII and Fe XXIV images; the image intensity is stronger than Fe XXII but weaker than Fe XXIV. The fields of view for the four images in Figure 4 differ slightly from one another.

© American Astronomical Society • Provided by the NASA Astrophysics Data System

1996ApJ...459..773D

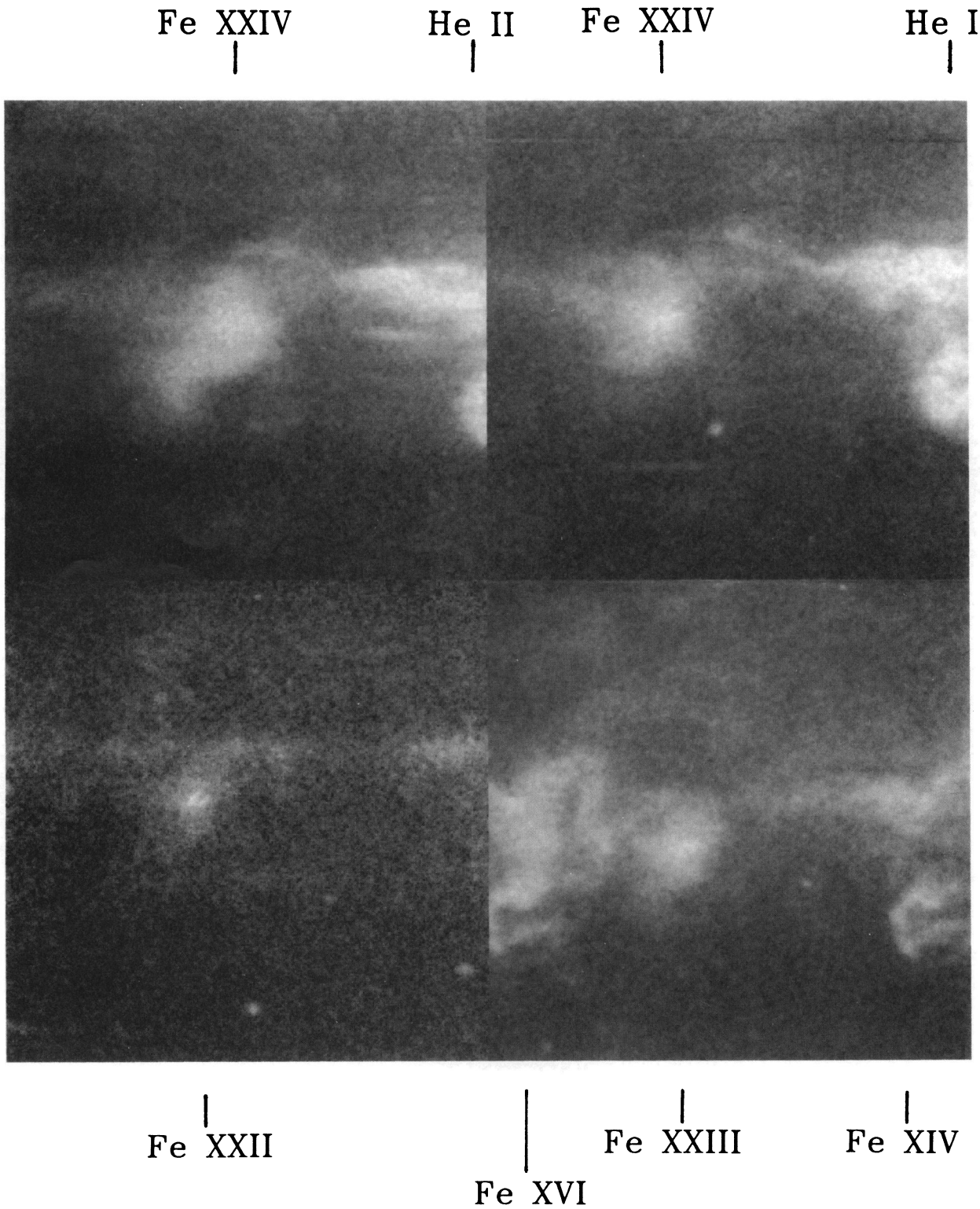

FIG. 4.—*Skylab* photographic density images of the June 15 flare. The upper left panel is an Fe XXIV image recorded during the rise phase; the upper right panel is an Fe XXIV image recorded near maximum flux. In these images, the Fe XXIV flare is near, and to the left of, panel center. The loop is oriented in roughly the up/down direction. The bright image at the right edge of each upper panel is part of the flare image in 256 Å He II. The solar dimensions of each panel are about 115,000 × 115,000 km^2. In the Fe XXIV upper right panel image, the loop top interacts with another faint loop oriented approximately in the left/right direction. This faint loop is seen extending to the left of the loop top. An Fe XXII image is shown in the lower left panel, and an Fe XXIII image is shown in the lower right panel. The Fe XXIII panel also includes images in Fe XIV and Fe XVI lines. The fields of view of the four panels differ slightly from one another, and the apparent image intensities have been adjusted arbitrarily for optimum display purposes. The wavelengths of the spectral images are as follows: He II, 303.78 Å; Fe XIV, 264.79 Å; Fe XVI, 262.98 Å; Fe XXII, 247.19 Å; Fe XXIII, 263.76 Å; Fe XXIV, 255.10 Å.

DOSCHEK & FELDMAN (see 459, 775)

© American Astronomical Society • Provided by the NASA Astrophysics Data System

1996ApJ...459..773D

3. ANALYSIS OF *SKYLAB* SPECTROHELIOGRAMS

Because the *Skylab* flare images were recorded on film, the film density must be transformed to photon intensity. An absolute intensity is not required because it is only the ratios of the intensities of the Fe XXII and Fe XXIII lines to the Fe XXIV line intensity that is important in our analysis. The film calibration curve was made using lines from spectra of different exposure times. Lines were chosen that did not vary intrinsically by a significant amount during the exposures. A one-dimensional slice through the most intense portions of the Fe images was chosen for analysis. Only images for which the film density was on the linear part of the film calibration curve were analyzed. Examples of Fe XXII and Fe XXIV slices are shown in Figure 5.

We derived line ratios for the brightest region in the loop top from a well-exposed spectroheliogram obtained at 14:14:36 UT, near the time of maximum broadband flux in the 0.5–3 Å region obtained from *Solrad* 9. At this time during typical compact flare evolution, the electron temperature as measured by BCS iron spectra is near its maximum value (e.g., Sterling, Doschek, & Pike 1994). An earlier spectroheliogram just before maximum flux is also available for the Fe XXIII and Fe XXIV lines and gives similar results for the Fe XXIII/Fe XXIV intensity ratio. (The Fe XXII line is too weak to measure in this earlier spectroheliogram.) The Fe XXII/Fe XXIV line intensity ratio (in ergs) in the 14:14:36 UT spectroheliogram is 0.11 and the Fe XXIII/Fe XXIV ratio is 0.43. These values also include approximately 20% corrections from instrument efficiency at the different wavelengths. The error in the line ratios is difficult to determine, but a rough estimate is about a factor of 1.5.

The Fe XXII/Fe XXIV and Fe XXIII/Fe XXIV intensity ratios can be related to ratios of emission measures at the temperatures of formation of Fe XXII, Fe XXIII, and Fe XXIV using standard techniques. Since flare densities are below the density necessary to significantly populate the ground configuration excited states of the Fe XXII, Fe XXIII, and Fe XXIV ions, there is no density sensitivity in line ratios and calculating the line intensities turns out to be simple, given radiative decay rates and excitation rate coefficients.

The intensity at Earth in a spectral line emitted by a cm^2 column along the line of sight is given by

$$I_{gu} = \frac{h\nu}{4\pi} \beta F(T_e) A_H \frac{N_H}{N_e} C_{gu}(T_e) B_{gu} N_e^2 \Delta h , \qquad (1)$$

where I_{gu} is the intensity (ergs cm^{-2} s^{-1} sr^{-1}) of a transition from upper level u to the ground level g, β is a measure of the width of the contribution function for the line, $F(T_e)$ is the fractional iron ion abundance at the temperature T_e, A_H is the iron abundance relative to hydrogen, C_{gu} is the electron impact excitation rate coefficient (cm^3 s^{-1}) for the transition from u to g, B_{gu} is the branching ratio from level u to level g, N_H is the number density of hydrogen, N_e is the electron density, and Δh is the path length of emission along a line of sight through the image. The ratio of $N_e^2 \Delta h$ for any two iron lines is equivalent to the emission measure ratio along the lines of sight intercepted by the slice through the images.

If the source is known to be multithermal and the temperature range spans a significant part of the contribution function, then the quantity β is 0.80 for the Fe XXII line, 0.94 for the Fe XXIII line, and 1.5 for the Fe XXIV line (Feldman et

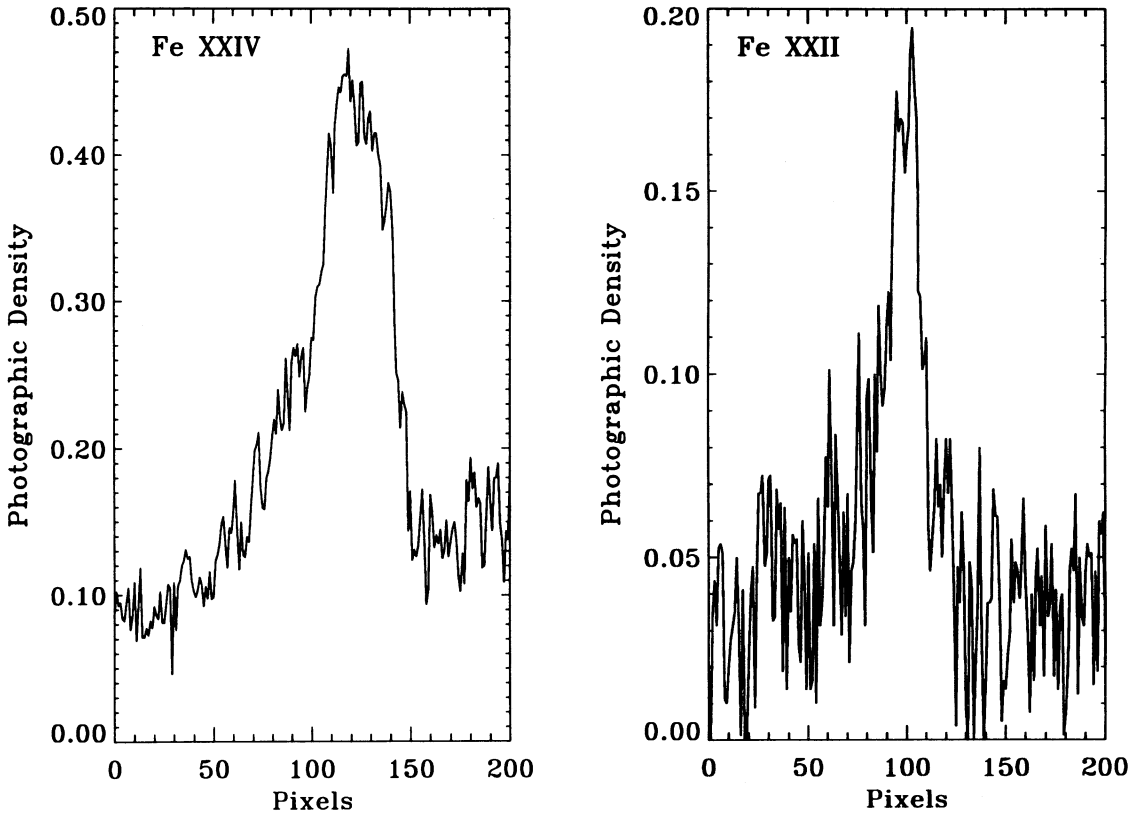

FIG. 5.—Examples of slices through the bright loop tops of the Fe XXII and Fe XXIV images. The one-dimensional slices are equivalent to spectral lines obtained with a slit spectrograph. Each pixel is equivalent to 8.322 mÅ in wavelength and 450 km in spatial extent.

© American Astronomical Society • Provided by the NASA Astrophysics Data System

1996ApJ...459..773D

al. 1992). However, if the source is assumed to be isothermal, then $\beta = 1$ for all lines.

The excitation rate coefficients for Fe XXII were obtained from Mason & Storey (1980) and from Zhang, Graziani, & Pradhan (1994). The earlier calculations are distorted wave; the later ones are close coupling calculations. Both sets of calculations agree very well for the 247 Å line. The excitation rate coefficient for the Fe XXIII intersystem line was obtained from close coupling calculations of Keenan et al. (1993). Excitation rate coefficients for the Fe XXIV line were obtained from Hayes (1979). Values for $F(T_e)$ were obtained from Arnaud & Rothenflug (1985) and Arnaud & Raymond (1992). The branching ratio B is 1 for the Fe XXIII and Fe XXIV lines and is 0.87 for the Fe XXII line. The Fe XXII value is based on radiative data in Mason & Storey (1980).

The theoretical intensity ratio of either Fe XXII/Fe XXIV or Fe XXIII/Fe XXIV is given by

$$R = \frac{B_i}{B_{255}} \frac{h\nu_i}{h\nu_{255}} \frac{F(T_e)_i}{F(T_e)_{255}} \frac{C_{gu}(T_e)_i}{C_{gu}(T_e)_{255}} \frac{\beta_i}{\beta_{255}} \frac{(N_e^2 \Delta h)_i}{(N_e^2 \Delta h)_{255}}, \quad (2)$$

where the subscript i refers to either the Fe XXII or the Fe XXIII line. The intensity ratio depends on both temperature and the line-of-sight emission measure ratio. The intensity ratios given in Figure 3 were obtained from equation (2) assuming an isothermal source, i.e., $\beta = 1$.

4. RESULTS

The experimental Fe XXII/Fe XXIV and Fe XXIII/Fe XXIV intensity ratios given in § 3 can be substituted into equation (2). To proceed further, assumptions about either the temperature or emission measure ratios must be made. If we assume that the source is isothermal, then the emission measure ratio is the same for all lines, the ratios of β values are unity, and equation (2) gives values for the ratio of the product of ion abundances and excitation rates, i.e., the ratio of contribution functions. Using the atomic data referenced, the isothermal assumption gives Fe XXII/Fe XXIV temperatures of 9.8×10^6 K and 12.3×10^6 K near flare maximum intensity, assuming Arnaud & Rothenflug and Arnaud & Raymond ionization balances, respectively. The corresponding Fe XXIII/Fe XXIV temperatures are 9.2×10^6 K and 11.3×10^6 K. Although the Fe XXII/Fe XXIII and Fe XXIII/Fe XXIV temperatures are somewhat different, they are close enough that it cannot be said with certainty that a multithermal source is implied, given the uncertainties in the atomic data. However, all these temperatures are about equal to or even somewhat lower than the SXT temperatures for bright loop tops, and therefore they appear questionable, as discussed in § 1. Nevertheless, without the BCS results the temperatures might be possible because the Fe XXIV line does emit significantly at temperatures near 10×10^6 K. Errors of a factor of 1.5 in the line ratios can only increase the temperatures by about 1×10^6 K.

If the plasma is assumed to be isothermal with a temperature significantly different from about 10×10^6 K, then equation (2) is only valid if there is an inaccuracy in the atomic physics. The size of the inaccuracy can be roughly estimated from Figure 2. For example, if a temperature of about 20×10^6 K is assumed for the bright loop top, i.e., a temperature typical for BCS Fe XXV spectra, then equation (2) gives values for the contribution function ratios calculated from Arnaud & Rothenflug (1985) that are about a factor of 30 greater than calculated using the atomic physics. This discrepancy is too large to be due to inaccuracies in the atomic physics, and thus it can be ruled out.

We conclude that an isothermal assumption will not yield a result that is consistent with results derived from BCS and previously obtained X-ray spectra. A possible explanation is that the loop top plasma is multithermal. Some support for this conclusion is obtained from the Ca XVII line near 192 Å that is also present in the spectroheliograms. The maximum emitting efficiency of the Ca XVII transition is near 6×10^6 K, well below the iron line temperatures. Nevertheless, Ca XVII emission is observed to be apparently co-spatial with the much higher temperature iron line emission, although the Ca XVII image is not concentrated at the loop top and appears as an extended loop. The Ca XVII emission at the same apparent location as the bright loop top could only arise in the loop top if the loop top were multithermal along the line of sight.

The simplest multithermal assumption is to assume that the Fe XXII, Fe XXIII, and Fe XXIV lines are emitted at the temperatures corresponding to the maxima of their contribution functions. This assumption does not rule out higher or lower temperatures; it simply specifies an average temperature for the three spectral lines, as would be assumed in an emission measure distribution analysis using many spectral lines emitted over a broad temperature range. The average temperatures for the Fe XXII, Fe XXIII, and Fe XXIV lines are 12×10^6 K, 13.6×10^6 K, and 17×10^6 K, respectively, for the Arnaud & Raymond (1992) ionization balance. The corresponding values obtained by adopting Arnaud & Rothenflug (1985) are 10.2×10^6 K, 12.6×10^6 K, and 14×10^6 K.

Using the contribution function values of β given above in equation (2), we obtain, assuming Arnaud & Raymond equilibrium, a 12×10^6 K to 17×10^6 K emission measure ratio equal to 3.8, i.e., this emission measure ratio is deduced from the Fe XXII/Fe XXIV intensity ratio. Adopting Arnaud & Rothenflug, we obtain a value equal to 5.6 for the corresponding 10.2×10^6 K to 14×10^6 K emission measure ratio. Similarly, from the Fe XXIII/Fe XXIV intensity ratio we derive a 13.6×10^6 K to 17×10^6 K emission measure ratio equal to 3.8 using Arnaud & Raymond and equal to 5.0 using Arnaud & Rothenflug for the corresponding 12.6×10^6 K to 14×10^6 K emission measure ratio.

All the above ratios are rather large, regardless of which ionization balance is adopted, and, under the multithermal assumption used to derive the ratios, they imply that there is considerable cool plasma along the line of sight through the loop top, as well as higher temperature plasma. More spectral lines from ions formed over a much broader temperature range are needed to determine an extended emission measure distribution.

If the conclusion that the June 15 flare bright loop-top region is multithermal were also true for most flares with bright loop tops, then the differences in SXT and BCS temperatures can at least qualitatively be explained as due to the different temperature sensitivities of the two instruments. Since SXT is sensitive to lower temperature plasmas than the BCS iron line spectrometer, the derived SXT temperatures for the bright loop top would generally be less than the BCS iron line temperatures for the bright loop top.

The fact that the bright loop top is multithermal for at least one flare does not imply that the Fe XXV–emitting plasma must arise only in this region. However, it does allow the possibility that some 20×10^6 K plasma is in this

© American Astronomical Society • Provided by the NASA Astrophysics Data System

1996ApJ...459..773D

region, for now there is a reason that the SXT temperatures might be less than the BCS temperatures, even if all the emission were to arise in the bright loop top. This also implies that if an isothermal loop top were found in *Yohkoh* data, then the SXT and BCS temperatures and emission measures for this source should be the same, provided there are no substantial instrumental or theoretical errors in data reduction techniques.

The close proximity of plasma at significantly different temperatures in the bright loop top implies that the bright region is composed of smaller structures below the spatial resolution of *Skylab* and *Yohkoh* instrumentation. The same conclusion was reached by Doschek et al. (1995), from an analysis of intensity variations within the bright regions in *Yohkoh* images. The small structures may represent "elementary bursts" of heating and cooling in many small regions within an overall volume that appears as a bright loop top. The stability of the overall bright region is still an unexplained problem.

The EUV analysis above could be improved considerably if more high-temperature spectral flare lines were available, covering a broader temperature range than possible with just the Fe XXII and Fe XXIV lines. The *Skylab* instrument was limited in wavelength range to wavelengths greater than about 170 Å. But with the new multilayer optics technology now available, the wavelength range could be extended down to 90 Å, which would encompass strong lines of Fe XVIII through Fe XXIII, in addition to the iron lines available at the longer wavelengths.

G. A. D. acknowledges support from W-18218 NASA SR&T Grant from the Solar Physics branch of the Space Science Division. The authors thank K. P. Dere and H. E. Mason for help in obtaining the atomic physics data.

REFERENCES

Acton, L. W., et al. 1992, PASJ, 44, L71
Arnaud, M., & Raymond, J. 1992, ApJ, 398, 394
Arnaud, M., & Rothenflug, R. 1985, A&AS, 60, 425
Cheng, C.-C. 1977, Sol. Phys., 55, 413
Culhane, J. L., et al. 1991, Sol. Phys., 136, 89
Doschek, G. A. 1990, ApJS, 73, 117
———. 1994, in Proc. Kofu Symposium on New Look at the Sun with Emphasis on Advanced Observations of Coronal Dynamics and Flares, ed. S. Enome & T. Hirayama (Nobeyama Radio Obs. Rep. 360), 173
Doschek, G. A., Strong, K. T., & Tsuneta, S. 1995, ApJ, 440, 370
Feldman, U., Mandelbaum, P., Seely, J. F., Doschek, G. A., & Gursky, H. 1992, ApJS, 81, 387
Feldman, U., Seely, J. F., Doschek, G. A., Brown, C. M., Phillips, K. J. H., & Lang, J. 1995, ApJ, 446, 860
Feldman, U., Seely, J. F., Doschek, G. A., Strong, K. T., Acton, L. W., Uchida, Y., & Tsuneta, S. 1994, ApJ, 424, 444
Hayes, M. A. 1979, MNRAS, 189, 55p
Kahler, S. 1977, ApJ, 214, 891
Keenan, F. P., Conlon, E. S., Warren, G. A., Boone, A. W., & Norrington, P. H. 1993, ApJ, 406, 350
Mason, H. E., & Storey, P. J. 1980, MNRAS, 191, 631
McTiernan, J. M., Kane, S. R., Loran, J. M., Lemen, J. R., Acton, L. W., Hara, H., Tsuneta, S., & Kosugi, T. 1993, ApJ, 416, L91
Sterling, A. C., Doschek, G. A., & Pike, C. D. 1994, ApJ, 435, 898
Tousey, R., Bartoe, J.-D., F., Brueckner, G. E., & Purcell, J. D. 1977, Appl. Opt., 16, 870
Tsuneta, S., et al. 1991, Sol. Phys., 136, 37
Vorpahl, J. A., Tandberg-Hanssen, E., & Smith, J. B., Jr. 1977, ApJ, 212, 550
Widing, K. G., & Dere, K. P. 1977, Sol. Phys., 55, 431
Zhang, H. L., Graziani, M., & Pradhan, A. K. 1994, A&A, 283, 319

© American Astronomical Society • Provided by the NASA Astrophysics Data System